Astron. Astrophys. 173, 263–270 (1987)

ASTRONOMY
AND
ASTROPHYSICS

H_2O maser emission from stars in the IRAS point-source catalog

B. Zuckerman[1] **and K.Y. Lo**[2]

[1] Department of Astronomy, University of California, Los Angeles, CA 90024, USA
[2] Department of Astronomy, California Institute of Technology, Pasadena, CA 91125, USA

Received February 25, accepted July 7, 1986

Summary. We searched for H_2O masers toward 61 red stars in the IRAS point-source catalog. Ten H_2O maser sources, roughly equally divided between pre- and post-main-sequence stars, were detected. A few may be "transition objects" that are evolving rapidly from red giants to planetary nebulae. One of these IRAS 1634 − 3814, has a very large *positive* radial velocity, $V_{LSR} \sim 140\,km\,s^{-1}$, although it lies in a direction where differential galactic rotation would be expected to produce *negative* radial velocities. The H_2O radial velocities imply large kinematic distances for some of the stars.

Key words: millimeter lines – stars: pre-main – sequence – stars: late-type

1. Introduction

The IRAS point-source catalog contains many reasonably bright, very red objects whose nature is uncertain. Possible classifications include pre-main-sequence stars embedded in molecular clouds, evolved stars (including planetary nebulae), and even galaxies. We have carried out a search for H_2O maser emission from 61 objects. We were interested primarily in identifying post-main-sequence stars and our search list was tailored to exclude IRAS sources that were likely to be pre-main-sequence stars. These can be identified in the IRAS catalog as objects that peak at $\lambda \gtrsim 100\,\mu m$. Our candidates all peaked at $\lambda \lesssim 60\,\mu m$. Many of the objects that we searched are classified as oxygen-rich by the IRAS low-resolution spectrometer (LRS). We also searched many IRAS objects with broadband fluxes that peak near $60\,\mu m$. Most of these were too faint at shorter wavelengths to be included in the LRS catalog. Such objects (which are quite rare), if evolved stars, may be in a short-lived state of rapid evolution from red giant to planetary nebulae.

2. Equipment and observations

We used the 40-meter telescope of the Owens Valley Radio Observatory equipped with a single-channel maser receiver. At the frequency (22235.08 MHz) of the 6_{16} to 5_{23} transition of H_2O, the system temperature was approximately 60 K at the zenith and the full half-power beamwidth of the antenna was 107″. The "back end" consisted of a 512-channel acousto-optic spectrometer (AOS) that had a total bandwidth of 100 MHz ($1331\,km\,s^{-1}$), so that the channel spacing was 195.3 kHz ($2.6\,km\,s^{-1}$), which is very nearly the resolution. As may be seen from the figures, this is insufficient to resolve many of the features that we detected, but is somewhat compensated for by the large velocity coverage possible with the OVRO AOS.

The data were obtained in July and August, 1985, by switching the telescope between a star and a reference position (typically, 5′ away in azimuth) at a rate of $\frac{1}{120}$ Hz and subtracting the off-source spectra from the on-source spectra. Total integration times, including time spent at the reference position, varied, typically, between 24 and 48 minutes for all stars that had not been previously detected in H_2O maser emission.

The data are summarized in Tables 1 and 2. The first column gives the source designation usually from either the IRAS or the Revised Air Force Geophysical Laboratory catalog (Price and Murdock 1983). The 1950 epoch positions listed in both tables are often good to a few arc seconds and, in any event, are good to a small fraction of the beamwidth of the 40-m telescope. The fourth and fifth columns are galactic longitude and latitude. The sixth column in both tables is peak flux in the line in Jy corrected for all telescope and atmospheric losses. We estimate that errors in T_B are probably approximately 20% (dominated by calibration errors). In Table 1, the seventh column gives V_{LSR}, the radial velocity (at peak line intensity) with respect to the local standard of rest. Many features are unresolved. Additional discussion of spectra may be found in Sect. 3.

Spectra of the ten newly detected H_2O sources are shown in Fig. 1. In Fig. 2 we display a spectrum that we obtained of IRAS 1913 + 2131 which was detected previously by Engels et al. (1984). We confirm the remarkably large velocity spread of H_2O maser features that they measured. However, the radial velocities of the H_2O features in our Fig. 2 disagree by approximately $3\,km\,s^{-1}$ with the velocities that they reported (see the caption to Fig. 2 for details). We do not understand the reason for this discrepancy. To check that our own measurements were not obviously systematically in error, we compared the radial velocity that we measured for two reasonably "standard" H_2O sources against previous observations.

For W Hya, we measured a strong H_2O feature at $V_{LSR} = 40.8\,km\,s^{-1}$ which may be compared with velocities of $42\,km\,s^{-1}$ and $39\,km\,s^{-1}$ given by Engels (1979) and of 40.6 and $38.6\,km\,s^{-1}$ measured by Spencer et al. (1979). Toward Orion we measured

Send offprint requests to: B. Zuckerman

Table 1. H_2O maser sources

Object (1)	α 1950 (2)	δ 1950 (3)	ℓ (4)	b (5)	F(Jy) (6)	V_{LSR}(km/s) (7)
IRAS 0239+6244	$2^h39^m30.^s6$	62°44'22"	135	2.8	10.5	- 69.8
IRAS 0436+2547	4 36 09.4	25 47 26	174	-13.7	9.8	11.8
BC Tau (AFGL 5171)	5 50 41.0	24 14 11	185	- 0.9	1.0	6.6
AFGL 5201	6 31 58.4	- 5 01 13	215	- 6.1	2.3	- 59.2
AFGL 1141	7 30 47.6	30 37 13	189	21.9	9.0	- 3.9
					1.1	17.1
IRAS 1634-3814	16 34 17.1	-38 14 18	344	5.8	1.3	143.5
					0.6	135.6
IRAS 1956+3423	19 56 38.1	34 23 20	71	2.7	2.7	- 40.8
IRAS 2014+3526	20 14 27.6	35 26 47	74	0.2	14.0	- 72.4
U Equ	20 54 45.0	2 47 10	51	-26.1	3.6	- 75.0
IRAS 2315+5912	23 15 08.6	59 12 25	111	- 1.2	12.5	- 51.3
					3.0	- 67.1

Table 2. Sources without H_2O masers

Object (1)	α 1950 (2)	δ 1950 (3)	ℓ (4)	b (5)	F(Jy) (6)
AFGL 190	$1^h14^m26.^s3$	66°58'08"	125	4.5	<0.3
IRAS 0243+6018	2 43 24.5	60 18 12	137	0.8	<0.3
IRAS 0320+5459	3 20 11.8	54 59 37	144	- 1.5	<0.3
AFGL 5093	3 20 41.6	65 21 31	138	7.3	<0.3
V Eri	4 02 01.6	-15 51 39	209	-44.0	<0.3
IRAS 0426+3550	4 26 57.2	35 50 28	165	- 8.5	<0.3
IRC+60144	4 30 45.9	62 10 12	146	9.9	<0.3
AFGL 5134	4 57 35.4	12 51 42	188	-17.6	<0.3
IRAS 0527+2517	5 27 22.2	25 17 41	181	- 4.8	<0.3
IRAS 0530+3029	5 30 32.0	30 29 03	177	- 1.3	<0.4
IRC+50149	5 36 08.3	46 44 10	164	8.3	<0.3
IRAS 0538-0728	5 38 02.7	- 7 28 59	212	-19.2	<0.3
IRC+40149	5 55 58.2	38 25 28	173	7.3	<0.3
IRAS 0713+1005	7 13 25.4	10 05 08	207	10.0	<0.4
AFGL 5235	7 31 11.5	-22 04 25	237	- 1.3	<0.2
IRAS 0733-1842	7 33 28.0	-18 42 17	235	0.8	<0.4
IRAS 0743-3750	7 43 28.3	-37 50 46	252	- 6.7	<0.3
AR Pup	8 01 10.9	-36 27 21	253	- 3.0	$\lesssim$0.7

Table 2 (continued)

Object	α 1950	δ 1950	ℓ	b	F(Jy)
(1)	(2)	(3)	(4)	(5)	(6)
IRAS 0818+5314	8 18 59.7	53 14 27	165	34.9	<0.6
IRAS 0857+3915	8 57 13.0	39 15 39	183	41	<0.3
SW Vir	13 11 29.7	- 2 32 33	314	59.6	<0.3
IRAS 1512-3658	$15^h12^m37^s.5$	-36°58'15"	332	17.3	<0.2
X Her	16 01 08.8	47 22 36	75	47.8	<0.2
NGC 6302	17 10 21.3	-37 02 38	350	1.1	<0.3
AFGL 6815S	17 15 04.6	-32 24 15	354	3.0	<0.3
AFGL 5379	17 41 07.4	-31 54 24	357	- 1.3	<0.3
AFGL 5384	17 43 40.7	50 03 47	77	30.9	≲0.4
IRAS 1753-0941	17 53 07.9	- 9 41 00	18	7.7	<0.3
IRAS 1755-1742	17 55 39.9	-17 42 18	11	3.2	<0.3
IRAS 1809+2704	18 09 30.9	27 04 28	54	20.2	<0.3
AFGL 5466	18 16 13.0	- 2 46 46	27	6.0	<0.3
IRAS 1818-1623	18 18 25.5	-16 23 56	15	- 1.0	<0.4
AFGL 5501	18 29 51.2	-21 11 54	12	- 5.6	<0.3
IRAS 1831-2834	18 31 03.7	-28 34 46	5	- 9.2	<0.3
AFGL 2199	18 33 19.6	5 33 17	36	6.0	<0.2
AFGL 2298	18 57 41.6	3 41 31	37	- 0.3	<0.3
VV CrA	18 59 43.9	-37 17 16	0	-18.2	<0.3
V342 Sgr	19 09 21.1	-32 56 05	5	-18.4	<0.3
AFGL 2343	19 11 25.0	0 02 18	36	- 4.9	<0.2
IRAS 1917+1511	19 17 17.4	15 11 06	50	0.9	<0.3
IRAS 1919+1526	19 18 19.0	15 26 59	50	0.8	<0.3
IRAS 1935+2030	19 35 12.6	20 30 06	56	- 0.3	≲0.5
IRAS 2002+3910	20 02 48.0	39 10 03	75	4.2	<0.3
AFGL 4259	$20^h04^m18^s.1$	26°53'30"	65	- 2.7	<0.3
IRAS 2131+5631	21 31 50.1	56 31 13	98	3.7	<0.2
IRAS 2155+6204	21 55 29.6	62 04 24	104	6.0	<0.4
IRAS 2203+5306	22 03 40.0	53 06 55	100	- 1.8	<0.4
IRAS 2227+5435	22 27 13.2	54 35 41	103	- 2.5	<0.4
IRAS 2255+6140	22 55 11.6	61 40 00	110	2.0	<0.2
IRAS 2326+6854	23 26 49.7	68 54 24	116	7.5	<0.3
IRAS 2332+6545	23 32 06.2	65 45 15	115	4.3	<0.3

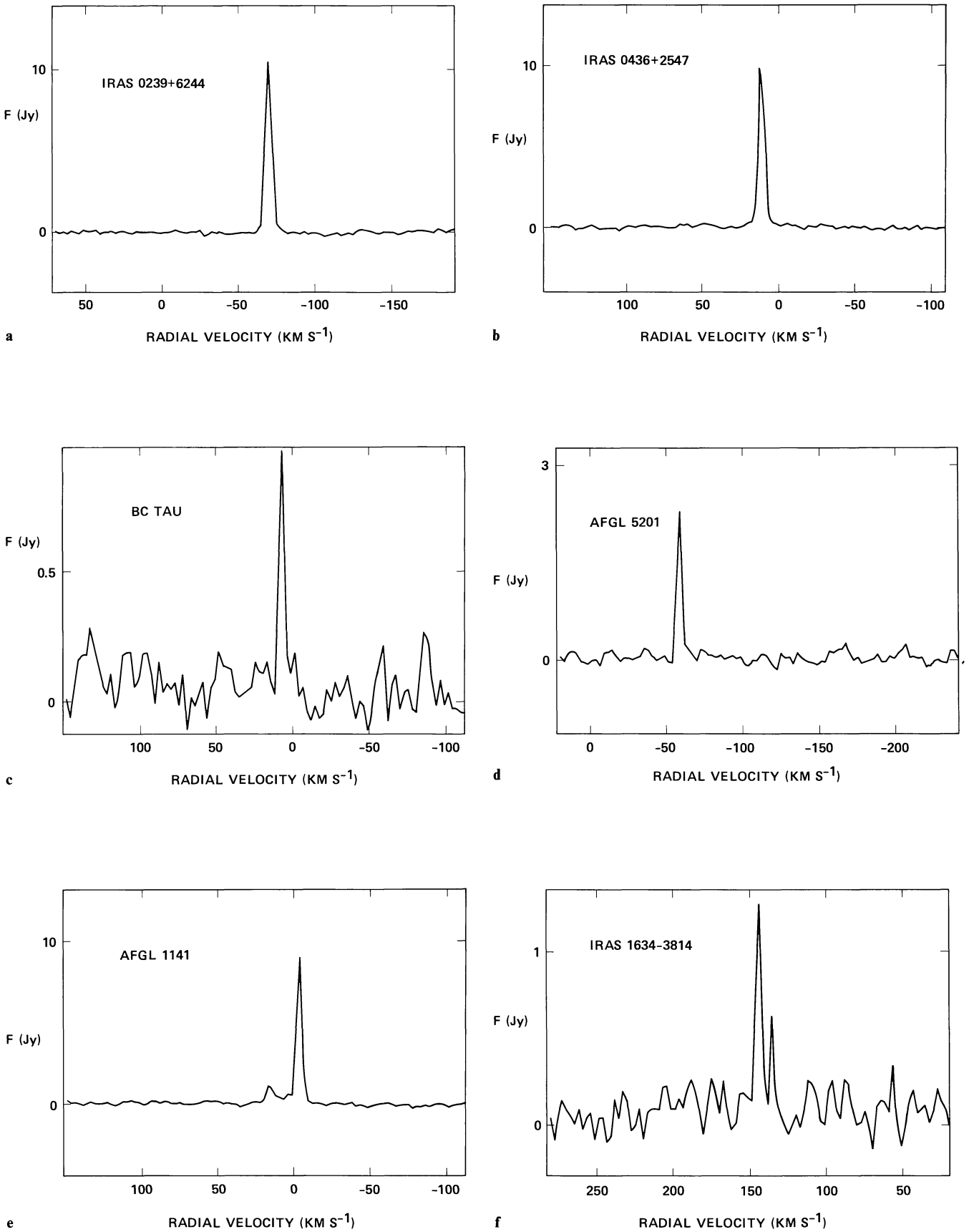

Fig. 1a-j. H_2O maser spectra for the ten sources in Table 1. The ordinate is flux in Janskys, the abscissa is radial velocity relative to the local standard of rest (V_{LSR})

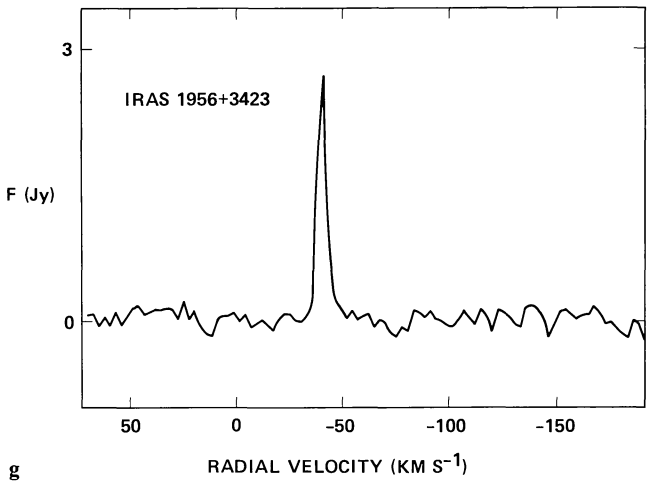

g

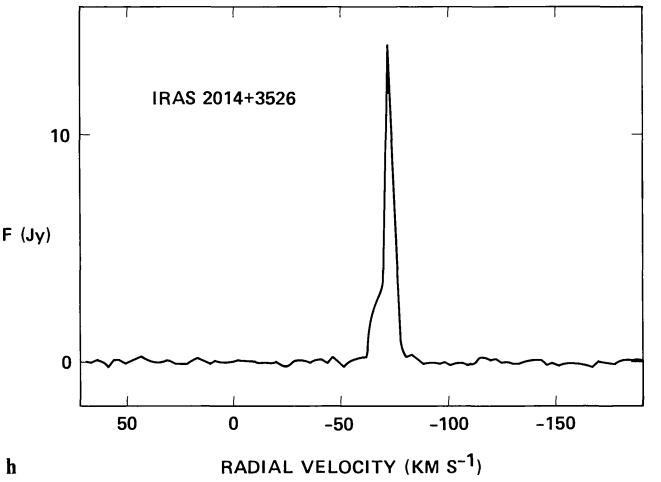

h

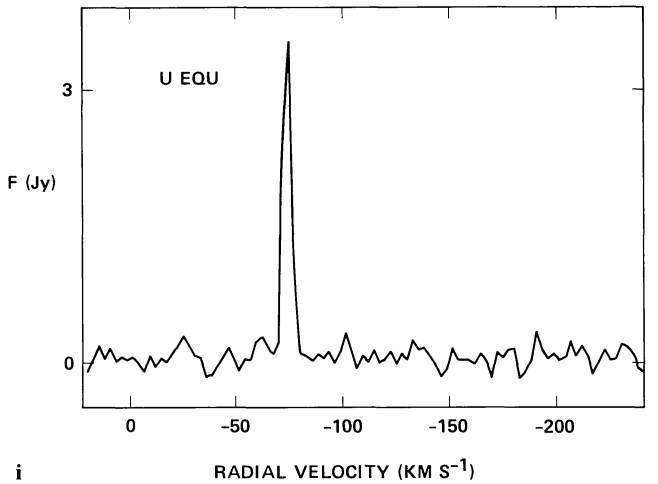

i

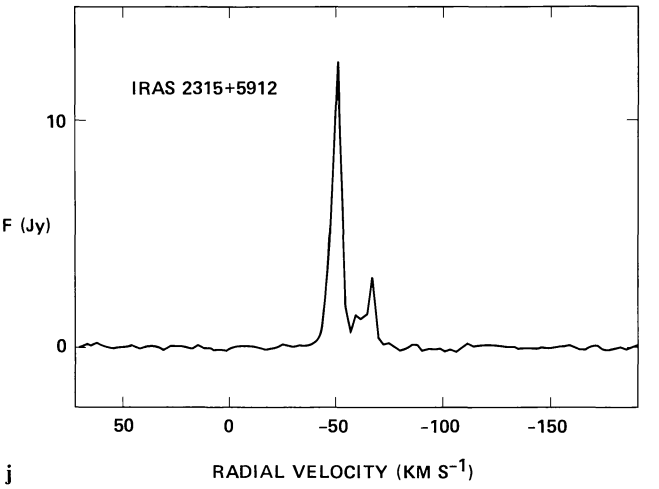

j

Fig. 1 (continued)

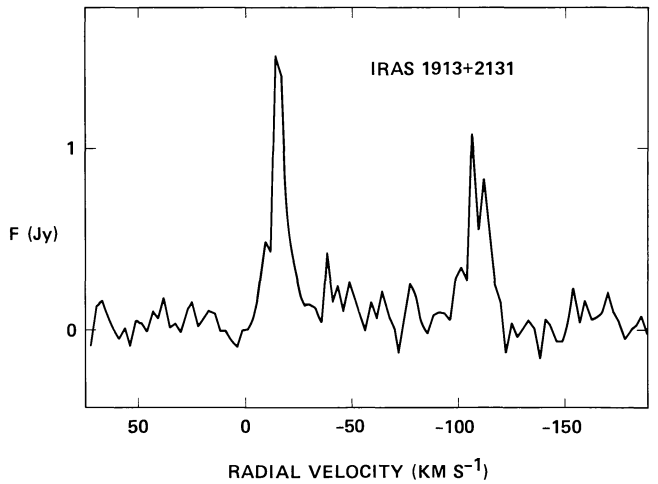

Fig. 2. H_2O maser spectrum of IRAS 1913+2131. The ordinate and abscissa are the same as in Fig. 1. The three peaks evident in this spectrum are at −14.5, −106.6, and −111.9 km s^{-1}, whereas Engels et al. (1984) report −18.8, −111.5 and −113.5 km s^{-1}. See Sect. 2 for discussion of this discrepancy

$V_{LSR} = 9.2\,km\,s^{-1}$ for the "super maser" feature for which Reid and Moran (1981) give $V_{LSR} = 8.1\,km\,s^{-1}$.

Recently, Engels (private communication, 1986), has suggested to us that velocity differences may be due to intrinsic variations in the source rather than measurement errors. This idea could be checked with future observations.

3. Individual stars

In this section we use the radial velocities of the H_2O masers to derive kinematic distances and bolometric luminosities for stars listed in Table 1 and located fairly close to the galactic plane. At these kinematic distances, some of the maser stars would be located a few hundred parsecs or more from the plane. Such stars might, conceivably, be "runaways" that have relatively large peculiar velocities which might invalidate distances that are derived using a standard model for galactic rotation. A case in point is AFGL 2343 (see Sect. 3.2.1 below and Zuckerman and Dyck 1986b) which may be a runaway supergiant. Because supergiants have very short main-sequence lifetimes, the peculiar velocity of AFGL 2343 perpendicular to the galactic plane must be large for

it to have reached its current galactic latitude, assuming that it was born in the plane. IRAS 1634 − 3814 (see Sect. 3.1.6) also might be a runaway star.

During the past few decades there has been substantial disagreement on the distance (R_0) between the Sun and the galactic center and on the circular velocity ($\omega_0 R_0$) of the Sun about the galactic center. A comprehensive, recent review of pertinent material by Kerr and Lynden-Bell (1985) suggests that the values assumed by Kerr and Westerhout (1965) (i.e., $R_0 = 8.2$ kpc and $\omega_0 R_0 = 216\,\mathrm{km\,s^{-1}}$) are close to the "best" values implied by recent research. Therefore, for stars that lie inside the solar circle, all kinematic distances quoted below are based on the rotation curve of Kerr and Westerhout (1965). Outside 8.2 kpc, we assume a flat rotation curve (preferred by Kerr and Lynden-Bell 1985).

3.1. H_2O masers detected

3.1.1. IRAS 0239 + 6244

This star displays a single unresolved H_2O feature. The broadband IRAS fluxes peak near 60 μm. The star was not measured with the LRS but Rieu et al. (1986) have detected a strong, narrow, J = 1 → 0, CO line toward the IRAS source, thereby implying that it is a pre-main-sequence star. The kinematic distance to the H_2O source is approximately 8 kpc and its luminosity, based on the IRAS 12 to 100 μm fluxes, is approximately $5\,10^4\,L_\odot$, consistent with an early B-type star.

3.1.2. IRAS 0436 + 2547

This star displays a single, unresolved H_2O feature. The broadband IRAS fluxes peak near 60 μm. We have no additional information on the star. If it is a pre-main-sequence star located inside the Taurus dark cloud, then at a distance of 150 pc it would have a minimum luminosity, based on the IRAS 12 to 100 μm fluxes, of approximately $3\,L_\odot$. A CO rotational spectrum might settle the matter.

3.1.3. BC Tau

This star displays a single, unresolved H_2O feature. The broadband IRAS fluxes peak near 60 μm. The star apparently has not previously been searched for any microwave maser emission (Bowers 1985, private communication).

3.1.4. AFGL 5201

This star displays a single, unresolved H_2O feature. The H_2O radial velocity indicates that AFGL 5201 has a large peculiar velocity.

3.1.5. AFGL 1141

H_2O emission is distributed over approximately $25\,\mathrm{km\,s^{-1}}$, implying an outflow velocity $\gtrsim 10\,\mathrm{km\,s^{-1}}$. This star was searched, without success, for J = 2 → 1 CO emission by Zuckerman et al. (1986). These results, plus the high galactic latitude, indicate that AFGL 1141 is an evolved oxygen-rich star in agreement with the classification in the RAFGL catalog.

3.1.6. IRAS 1634 − 3814

Two H_2O features are detected from this star. The radial velocity is remarkable: $+140\,\mathrm{km\,s^{-1}}$ in a direction where differential galactic rotation would produce negative radial velocities. Because of the peculiar V_{LSR}, we suspect that the star is located in the nuclear bulge. At a distance of 8 kpc, the IRAS 12 to 100 μm fluxes, which peak near 60 μm, imply a minimum luminosity of approximately $6\,10^4\,L_\odot$, placing the star, if it is evolved, at the very tip of the AGB. In December 1984, Zuckerman and Dyck (1986a) searched, without success, for J = 2 → 1 CO emission from this star. These data were limited and of poor quality but, even so, if IRAS 1634 − 3814 were a young, massive star embedded in a molecular cloud, then a CO line would have been expected. This negative result, combined with the large radial velocity and location out of the galactic plane (approximately 800 pc at 8 kpc), implies that the star is post-main-sequence. (An extragalactic origin for the H_2O maser is also, perhaps, not impossible).

3.1.7. IRAS 1956 + 3423

This star displays a single unresolved H_2O feature. The kinematic distance is approximately 9 kpc, which implies a minimum luminosity of approximately $6\,10^4\,L_\odot$ based on the IRAS 12 to 100 μm fluxes. Zuckerman and Dyck (1986b) searched, without success, for CO J = 1 → 0 emission from this star in June, 1985. This negative result suggests that the star is post-main-sequence. This agrees with the IRAS LRS designation and with the broadband IRAS colors which are indicative of an oxygen-rich evolved star (Zuckerman and Dyck 1986b). If so, apparently it is located very near to the tip of the AGB.

3.1.8. IRAS 2014 + 3526

The asymmetrical H_2O line is obviously a blend of at least two separate features. The kinematic distance is approximately 12 kpc, so the IRAS 12 to 100 μm fluxes (which peak near 60 μm) imply a minimum luminosity in excess of $10^5\,L_\odot$. The IRAS LRS designation was either an oxygen-rich evolved star with an extremely thick circumstellar envelope or a hot spot in a molecular cloud. If the kinematic luminosity is to be trusted, then the star is massive and pre-main sequence. Rieu et al. (1986) detected a strong, narrow, J = 1 → 0, CO line toward the IRAS source consistent with a pre-main-sequence classification. The galactic latitude of this massive star is small (see Table 1). However, because of the warp of the galaxy in this direction, the star lies a few hundred parsecs below the mid-plane of the neutral hydrogen at this location (see Fig. 2 in Henderson et al. 1982).

3.1.9. U Equ

This evolved star displays a single unresolved H_2O feature. It is located far from the galactic plane, and has a large peculiar velocity. For an oxygen-rich star it has an unusually large 60 μm IRAS flux relative to the 25 μm flux, somewhat similar to the star GX Mon which is discussed by Zuckerman and Dyck (1986b).

3.1.10. IRAS 2315 + 5912

H_2O emission is distributed over approximately $25\,\mathrm{km\,s^{-1}}$. The kinematic distance is approximately 6 kpc, so the IRAS 12 to 100 μm fluxes (which peak near 60 μm) imply a minimum luminosity of approximately $\sim 6\,10^4\,L_\odot$. The IRAS LRS designation indicates an evolved oxygen-rich star. However, Rieu et al. (1986) detected a very strong, narrow, J = 1 → 0, CO line toward the IRAS source indicative of a pre-main-sequence star.

3.2. H_2O masers not detected

3.2.1. AFGL 2343

This is a bright but very red IRAS source that is associated with a G-type star. Zuckerman and Dyck (1986b) detected a broad CO $J = 1 \rightarrow 0$ line in this direction at V_{LSR} approximately 105 km s^{-1}. If the star is at the kinematic distance of 6 kpc, then both the 12 to 100 μm luminosity and the large linewidth are consistent with a supergiant-class star perhaps similar to IRC + 10420. Since red, oxygen-rich supergiants often show H_2O maser emission, we searched in AFGL 2343 but detected nothing. The star is also not an HCN source (Claussen 1985, private communication). If it is oxygen-rich, as appears likely, then OH maser emission may be detectable.

3.2.2. AFGL 190

This star, tentatively identified as carbon-rich by Kleinmann et al. (1981), is classified as oxygen-rich in the IRAS LRS catalog. We examined the LRS spectrum and find that it is ambiguous as are the relative broadband IRAS colors at 12, 25 and 60 μm (Zuckerman and Dyck 1986b). These IRAS fluxes peak near 25 μm which is very unusual if the star is carbon-rich and of a late type. All searches for maser emission from AFGL 190 have been negative. After our H_2O observations were completed, Zuckerman and Dyck (1986b) detected HCN emission from AFGL 190 at a level that virtually assures that it is carbon-rich.

3.2.3. AFGL 2199

This star shows H_2O absorption bands near 2 μm (Joyce and Gillett 1985, private communication) and has been classified as oxygen-rich (Kleinmann et al. 1981). The broadband IRAS colors also suggest an O-rich star (Zuckerman and Dyck 1986b). However, the IRAS LRS spectrum is somewhat unusual, and, indeed, the classification is given as carbon-rich. All searches for maser emission from AFGL 2199 have been negative.

3.2.4. IRC + 60144

This star is classified as oxygen-rich in the RAFGL catalog (where it is mislisted as DO 28489 instead of DO 28389). However, the IRAS LRS designation is carbon-rich and, indeed, there is, apparently, an SiC feature present near 11 μm. The relative broadband IRAS colors are ambiguous (Zuckerman and Dyck 1986b). All searches for maser emission from IRC + 60144 have been negative. After our H_2O observations were completed, Zuckerman and Dyck (1986b) detected HCN emission from IRC + 60144 at a level that virtually assures that it is carbon rich.

3.2.5. NGC 6302

This is an unusual oxygen-and nitrogen-rich planetary nebula that may be associated with a detectable cloud of atomic hydrogen (Rodriguez et al. 1985). Zuckerman and Dyck (1986b) detected a CO $J = 1 \rightarrow 0$ line with a peculiar radial velocity in this direction. To perhaps clarify the situation we searched, unsuccessfully, for H_2O maser emission.

4. Discussion

Detection of H_2O or OH maser emission can help one to classify an IRAS source as a pre- or post-main-sequence star and as oxygen- (as opposed to carbon-) rich. For stars near the galactic plane, a fairly good kinematic distance can often be derived and, combined with the IRAS fluxes, a minimum bolometric luminosity calculated (see Sect. 3). For post-main-sequence stars, these IRAS fluxes can be converted into mass loss rates in dust ($\dot{M}_d$). A quantity of considerable interest is the mass loss rate in gas ($\dot{M}_g$) which, for AGB stars within approximately 2 kpc of the Sun, can be estimated from carbon monoxide millimeter emission (e.g., Knapp and Morris 1985; Zuckerman and Dyck 1986a). For more distant AGB stars, such as some of those detected in this survey, that are beyond the reach of the current crop of CO millimeter systems (Zuckerman 1985), only IRAS fluxes are available. There exist thousands of such stars. For these, if we know both the distance and the dust-to-gas abundance ratio, then we can calculate $\dot{M}_g$. The distance may be obtained within a factor of order 2 if one assumes a typical AGB bolometric luminosity $L_* \sim 10^4\, L_\odot$. However, since we are often interested in $R(\equiv \dot{M}_g v_\infty c/L_*)$, which is the ratio of the momentum in the wind to that in the radiation field (e.g., Jura 1983), the assumption of a standard L_* for all AGB stars introduces an error into the determination of R for an individual star. If a kinematic distance for a given star is determined via H_2O or OH maser emission, then the bolometric luminosity may be calculated rather than assumed. The *average* circumstellar dust-to-gas ratio may be "calibrated" by using nearby oxygen-rich stars for which $\dot{M}_g$ may be obtained from CO measurements (Sopka et al. 1985; Zuckerman 1985) and this average can then be applied to more distant stars for which only $\dot{M}_d$ is available. We now apply this technique to derive R for IRAS 1634 − 3814 and IRAS 1956 + 3423 which are unlikely to be detected easily in CO emission if they are as distant as we have argued in Sect. 3.

To calculate $\dot{M}_d$, we use the prescription outlined by Sopka et al. (1985), in particular their Eqs. (3) and (A1). We assume a dust outflow velocity of 15 km s^{-1}. To normalize the dust grain temperature distribution, we use their expression B3. An important parameter in the analysis is p, the grain emissivity index defined by $Q \propto \lambda^{-p}$, where Q is the emission efficiency of a given grain. For a modest sample of stars, most of which are carbon-rich, Sopka et al. (1985) argue that $p \sim 1.2$ between $10 < \lambda < 400\,\mu$m. The true situation is probably somewhat more complex since, according to Zuckerman and Dyck (1986b), IRAS data for O-rich AGB stars suggest that, between 25 and 60 μm, $p \sim 1.6$ which is larger, on the average, than p for C-rich stars by approximately 0.4. For IRAS 1634 − 3814, which has a peak flux near 60 μm and emits most of its energy in this range of wavelengths, we set $p = 1.4$ in expression A1 of Sopka et al. and expect that this choice of p will not be in error by more than ± 0.3. For IRAS 1956 + 3423, most of the energy is emitted between 12 and 25 μm and we use a slightly smaller value for $p = 1.25$ (Zuckerman and Dyck 1986b).

To evaluate $\dot{M}_d$, it is necessary to know the opacity, k_ν (cm^2 g^{-1}), at a given frequency. IRAS 1634 − 3814 is sufficiently red that, for any reasonable value of p, the 100 μm flux implies the largest $\dot{M}_d$ of any of the four IRAS wavebands. As we describe below, $\dot{M}_d$ implied by the 25 μm flux is substantially smaller. To estimate k_ν at 100 μm and at 25 μm, we assume $p = 1.5$ (Zuckerman and Dyck 1986b) and scale the 400 μm value of 20 cm^2 g^{-1} deduced by Sopka et al. (1985). Then k_ν (100 μm) = 160 cm^2 g^{-1} and k_ν (25 μm) = 1280 cm^2 g^{-1}. These values for k_ν are uncertain by at least a factor of 2. Errors in $\dot{M}_d$ that are introduced by uncertainties in p (as discussed in the preceding paragraph) are subsumed in these estimates of k_ν.

For IRAS 1956 + 3423 we calculate $\dot{M}_d = 3\,10^{-7}\,M_\odot$/yr based on the 60 μm flux (IRAS did not measure a 100 μm flux for this star). For IRAS 1634 − 3814 we calculate $\dot{M}_d = 1\,10^{-6}\,M_\odot$/yr and $1\,10^{-7}\,\dot{M}_\odot$/yr from the 100 μm and 25 μm fluxes, respectively. If IRAS 1634 − 3814 is 8 kpc from the Earth, then the dust that is radiating at 100 μm was ejected from the star a few thousand years before the dust that is radiating at 25 μm (assuming an outflow velocity $\sim 15\,\mathrm{km\,s^{-1}}$). If the mass loss is driven by radiation pressure on dust grains and the current luminosity of the star is $6\,10^4\,L_\odot$, then the stellar luminosity would have been well above the AGB limit a few thousand years ago. Since we regard this as unlikely, perhaps IRAS 1634 − 3814 is a high-velocity runaway star that is located considerably closer to the Earth than 8 kpc. Assuming $\dot{M}_g/\dot{M}_d = 200$, we calculate $R \sim 1$ for both IRAS 1956 + 3423 and IRAS 1634 − 3814, consistent with mass outflow driven by radiation pressure on dust grains (e.g., Jura 1983).

5. Conclusions

We have detected H_2O maser emission toward ten very red sources in the IRAS point source catalog. Because many of the H_2O masers have large radial velocities with respect to the local standard of rest, they are useful in establishing kinematic distances and luminosities for the associated IRAS sources. Many of these are unusual in that they have IRAS fluxes that peak at 60 μm wavelength. We argued that the majority are associated with pre-main-sequence stars. There are also many additional IRAS sources, Table 2, toward which we searched, unsuccessfully, for H_2O maser emission. A search of these sources for OH masers would be worthwhile.

Acknowledgements. We are very grateful to Dr. F.C. Gillett for supplying us with an early list of IRAS sources with peak fluxes near 60 μm. Dr. S. Scott and Mr. M. Hodges kindly provided assistance at the telescope. We thank Drs. P. Bowers and M. Jura for some useful comments, Dr. R.J. Sopka for assistance, and Drs. J.M. Cahn and L.E. Snyder for sending us a catalog of known stellar masers. We thank Mr. R.L. O'Daniel for editing and typing the manuscript. This research was supported in part by NSF Grants AST 83-18342 to UCLA and AST 84-12473 to Cal Tech.

Note added in proof: To clarify the nature of IRAS 1634-3814 we asked Dr. R.J. Maddalena to observe the source with the 43-meter antenna of the U.S. National Radio Astronomy Observatory. On 14 November 1986, he very kindly obtained a spectrum with $0.5\,\mathrm{km\,s^{-1}}$ spectral resolution that displayed an H_2O emission feature at $146.9\,\mathrm{km\,s^{-1}}$ having roughly the same intensity as the $143\,\mathrm{km\,s^{-1}}$ feature listed in Table 1. In addition, the 43-m spectrum indicates a weaker emission peak at 171.9 $\mathrm{km\,s^{-1}}$ with about one quarter of this intensity. This indicates, reasonably conclusively, that IRAS 1634-3814 is an evolved star with systemic velocity $\sim 160\,\mathrm{km\,s^{-1}}$ and outflow velocity ~ 13 $\mathrm{km\,s^{-1}}$. Also, at our request, Ms. L. Likkel kindly examined IRAS 1634-3814, also with the 43-m telescope, at the frequencies of the four 18-cm lines of OH. In early October 1986, no OH emission was detectable at or near the H_2O emission velocities although OH emission was detected at various other velocities (Likkel 1987, in preparation).

References

Engels, D.: 1979, *Astron. Astrophys. Suppl.* **36**, 337
Engels, D., Habing, H.J., Olnon, F.M., Schmid-Burgk, J., Walmsley, C.M.: 1984, *Astron. Astrophys.* **140**, L9
Henderson, A.P., Jackson, P.D., Kerr, F.J. 1982, *Astrophys. J.* **263**, 116
Jura, M.: 1983, *Astrophys. J.* **275**, 683
Kerr, F.J., Lynden-Bell, D. 1985, Report to Commission 33 of the IAU
Kerr, F.J., Westerhout, G.: 1965, in *Galactic Structure*, editors A. Blaauw, M. Schmidt, University of Chicago Press, p. 167
Kleinmann, S.G., Gillett, F.C., Joyce, R.R.: 1981, *Ann. Rev. Astron. Astrophys.* **19**, 411
Knapp, G.R., Morris, M.: 1985, *Astrophys. J.* **292**, 640
Price, S.D., Murdock, T.L.: 1983, The Revised AFGL Infrared Sky Survey Catalog, AFGL-TR-83-0161
Reid, M.J., Moran, J.M.: 1981, *Ann. Rev. Astron. Astrophys.* **19**, 231
Rieu, N.-Q., Zuckerman, B., Truang-Bach.: 1986, (in preparation)
Rodriguez, L.F., et al.: 1985, *Monthly Notices Roy. Astron. Soc.* **215**, 353
Spencer, J.H., Johnston, K.J., Moran, J.M., Reid, M.J., Walker, R.C.: 1979, *Astrophys. J.* **230**, 449
Sopka, R.J., Hildebrand, R., Jaffe, D.T., Gatley, I., Roellig, T., Werner, M., Jura, M., Zuckerman, B.: 1985, *Astrophys. J.* **294**, 242
Zuckerman, B.: 1985, in *First International IRAS Symposium: Light on Dark Matter*, ed. F. Israel, Reidel, Dordrecht
Zuckerman, B., Dyck, H.M.: 1986a, *Astrophys. J.* **304**, 394
Zuckerman, B., Dyck, H.M.: 1986b, *Astrophys. J.* (in press, December 1986)
Zuckerman, B., Dyck, H.M., Claussen, M.J.: 1986 *Astrophys. J.* **304**, 401